BJ www.biochemj.org

BJ Disease

Biochem. J. (2010) **429**, 473–483 (Printed in Great Britain) doi:10.1042/BJ20100155

online data

The potency of the fs260 connexin43 mutant to impair keratinocyte differentiation is distinct from other disease-linked connexin43 mutants

Jared M. CHURKO, Stephanie LANGLOIS, Xinyue PAN, Qing SHAO and Dale W. LAIRD[1]

Department of Anatomy and Cell Biology, University of Western Ontario, London, Ontario, Canada N6A 5C1

Although there are currently 62 mutants of Cx43 (connexin43) that can cause ODDD (oculodentodigital dysplasia), only two mutants have also been reported to cause palmar plantar hyperkeratosis. To determine how mutants of Cx43 can lead to this skin disease, REKs (rat epidermal keratinocytes) were engineered to express an ODDD-associated Cx43 mutant always linked to skin disease (fs260), an ODDD-linked Cx43 mutant which has been reported to sometimes cause skin disease (fs230), Cx43 mutants which cause ODDD only (G21R, G138R), a mouse Cx43 mutant linked to ODDD (G60S), a non-disease-linked truncated Cx43 mutant that is trapped in the endoplasmic reticulum (Δ244*) or full-length Cx43. When grown in organotypic cultures, of all the mutants investigated, only the fs260-expressing REKs consistently developed a thinner stratum corneum and expressed lower levels of Cx43, Cx26 and loricrin in comparison with REKs overexpressing wild-type Cx43. REKs expressing the fs260 mutant also developed a larger organotypic vital layer after acetone-induced injury and exhibited characteristics of parakeratosis. Collectively, our results suggest that the increased skin disease burden exhibited in ODDD patients harbouring the fs260 mutant is probably due to multiple additive effects cause by the mutant during epidermal differentiation.

Key words: connexin43, gap junction, keratinocyte, organotypic epidermis, palmar plantar hyperkeratosis.

INTRODUCTION

Direct cell-to-cell communication relies heavily on the passage of small molecules through gap junctions [1]. Structurally, gap junctions are composed of connexin proteins which oligomerize in the Golgi apparatus to form connexons [2]. Connexons are transported to the cell surface and dock with connexons from an adjacent cell to form functional channels [3]. Given that connexins and gap junctions have a half-life of only 1–5 h both *in vitro* and *in vivo*, constant regulatory control of connexin translation, oligomerization, delivery to the cell surface and assembly are all critical for the proper regulation of GJIC (gap junctional intercellular communication). When regulatory processes involved in the life cycle of connexins become disrupted, GJIC is compromised and disease may result. For example, disease-linked mutations in the gene encoding Cx43 (connexin43) have been shown to sequester endogenous and mutant Cx43 in intracellular compartments [4], and inhibit the passage of small molecules through gap junction channels and hemichannels [5,6]. Clinically, germ line mutations in nine connexin gene family members lead to human diseases that include skin diseases (e.g. Cx26, Cx43) [7], cataracts (e.g. Cx45, Cx50) [8], deafness (e.g. Cx26) [9], arrhythmias (e.g. Cx40, Cx43) [10], Charcot–Marie–Tooth disease (e.g. Cx32) [11] and ODDD (oculodentodigital dysplasia) (e.g. Cx43) [12].

ODDD was first described as a disease displaying craniofacial abnormalities (microphthalmia, dental anomalies, small nose and hypotrichosis), type III syndactyly and missing toe phalanges [13]. Since its initial characterization, spastic paraparesis, cerebral white matter abnormalities [14] and ectodermal abnormalities [12,15,16] have also been associated with ODDD. ODDD is a rare condition as less than 1000 cases having been fully documented, although now that the genetic link to the disease is known, the number of reported cases is likely to grow substantially [12]. To date, ODDD is associated with 62 familial or sporadic mutations in the gene encoding Cx43 with the majority (~85 %) being dominant missense mutations [12]. Functional assays employing some of these mutations have found that the mutants encoded are dominant-negative and result in a drastic reduction in normal Cx43 function [4,6]. These mutations are associated with a wide array of phenotypic outcomes and, generally, domain-specific mutations were not found to correlate with a specific ODDD symptom. For example, ODDD has been diagnosed in patients having mutations in the N-terminal end (e.g. Y17S and G21R), first extracellular loop (e.g. A40V, G60S and P59S), cytoplasmic loop (e.g. V96M and G138R), second extracellular loop (e.g. H194P) and C-terminal tail (e.g. fs230 and fs260) [12]. Although most of these mutations often result in syndactyly and cranial facial abnormalities, two ODDD mutants that truncate the C-terminal tail (fs230 and fs260) have been reported to additionally cause the skin disease palmar plantar hyperkeratosis [17,18]. Although both of these mutants have been reported to cause palmar plantar hyperkeratosis, a newly identified patient expressing the fs230 mutant did not exhibit this skin disease phenotype [19]. Importantly, the fs260 mutant has a polypeptide extension of 46 non-connexin-related amino acids before a stop codon is encountered, whereas the fs230 mutant only has a six-amino-acid extension prior to reaching a stop codon [17]. Thus, although these two mutants both lack the C-terminal tail, they differ extensively in non-connexin polypeptide sequence that may contribute to the disease phenotype in the skin.

Palmar plantar hyperkeratosis has been linked to a wide array of abnormal processes. Palmar plantar hyperkeratosis involves a thickening of the epidermis in the friction and weight-bearing

Abbreviations used: Cx43, connexin43; DAPI, 4′,6-diamidino-2-phenylindole; DMEM, Dulbecco's modified Eagle's medium; EGFP, enhanced green fluorescent protein; GFP, green fluorescent protein; GJIC, gap junctional intercellular communication; HBSS, Hanks balanced salt solution; ODDD, oculodentodigital dysplasia; PDI, protein disulfide isomerase; REK, rat epidermal keratinocyte.

[1] To whom correspondence should be addressed (email dale.laird@schulich.uwo.ca).

surfaces of the palms and the plantar region of the feet. Congenitally, palmar plantar hyperkeratosis can also be caused by mutations in the genes which code for epidermal proteins. Mutant keratin 1, keratin 10 [20], Cx26 (Vohwinkel's syndrome) [21] and desmosomal proteins [22] have all been reported to be genetically linked to palmar plantar hyperkeratosis. In the case of Cx43 mutations, it is currently not known whether the mechanism by which Cx43 mutants cause palmar plantar hyperkeratosis is somehow associated to these other skin disease-linked proteins. However, it has previously been shown that a mutant Cx26 which causes palmar plantar hyperkeratosis can have transdominant effects on Cx43 [23]. Thus it may also be possible that mutant Cx43 causes palmar plantar hyperkeratosis through transdominant effects on Cx26. It is also reasonable to assume that, since keratins, desmosomes and tight junctions are all responsible for maintaining the integrity of the epidermal barrier, Cx43 mutants that disrupt any one of these components may lead to disruptions in the membrane barrier and contribute to palmar plantar hyperkeratosis. In the present study we examined the mechanism by which mutations in the gene encoding Cx43 can affect skin differentiation and how some mutations associated with ODDD, but not others, can lead to skin disease.

MATERIALS AND METHODS

Cell lines

REKs (rat epidermal keratinocytes) were originally characterized by Baden and Kubilus [24] and were grown in REK growth medium composed of DMEM (Dulbecco's modified Eagle's medium) supplemented with 2 mM L-glutamine, 10 % fetal bovine serum, 100 μg/ml streptomycin and 100 units/ml penicillin.

Transfection and infection

Transfection of packaging 293 GPG cells was carried out using the previously reported and characterized AP2 vector encoding full-length Cx43 tagged with GFP (green fluorescent protein) (Cx43–GFP) or the Cx43 mutants G21R, G60S, G138R, Δ244 with mutations G58R and S158A (Δ244*) [25] and fs260. In addition, a fs230 mutation was also created using the Qiagen QuikChange site-directed mutagenesis kit with the primers 5′-ATCATTGAACTCTTCTGTTTTCTTCAAGGGCGTTAAGGATCGGG (forward) and 5′-CCCGATCCTTAACGCCCTTGAAGAAAACAGAAGAGTTCAATGAT (reverse) for human Cx43 pcDNA3.1. Untagged fs230 pcDNA3.1 was used to rule out effects caused by the GFP tag. The mutant fs230 sequence was then fused in frame into a EGFP (enhanced GFP)-N1 (Clontech) vector and further incorporated into a AP2 vector using the primers 5′-ATCTCGACATGGGTGACTGGAGCGC (forward) and 5′- GGTGGATCCGGACGCCCTTGAAGAA (reverse). The fs230–GFP mutant construct encodes the first 229 amino acids of Cx43, six amino acids resulting from the frame shift (CFLEGR), seven amino acid linkers (PDPPLAT) and the EGFP protein sequence.

To perform transfections of packaging 293 cells, 2.5 ml of Opti-MEM was placed into two separate 5 ml tubes. The AP2 vector (10 μg) was placed into one tube while 15 μl of Lipofectamine™ 2000 was added to the second tube. Within 5 min, both tubes were combined and were incubated for 20 min. Packaging cells in a 100-mm-diameter culture dish were then washed twice in Opti-MEM medium and the combined Lipofectamine™/AP2 vector solution was administered on to the growing packaging 293 cells. After 6 h, the Lipofectamine™ solution was aspirated and the packaging cells were grown overnight in low-glucose DMEM supplemented with 10 % fetal bovine serum, 10 mg/ml tetracycline and 20 mg/ml G418. The next day, 5 ml of fresh REK growth medium was placed on to the transfected packaging cells and viral collections were made every day for four days. Collected viral medium was concentrated by centrifugation in sealed 5.1 ml tubes for 90 min in a Beckman TL100 ultracentrifuge at 4 °C at 25 000 rev./min (Beckman Instruments). After centrifugation, the viral pellet was resuspended in 0.5 ml of REK growth medium and stored at − 80 °C.

REKs were grown to 20 % confluence and the viron-containing supernatant was exposed to the cells overnight and 5 μg/ml polybrene was also added to the medium. The next day, fresh medium was placed on to each REK-infected cell line and these cell lines were passed five times before being visualized under a confocal microscope. Each REK cell line was successfully transduced, with 95–100 % of all cells expressing the Cx43 mutants.

Antibodies and imaging

Immunofluorescence was performed by incubating the cells overnight with an anti-C-terminal Cx43 antibody (P4G9; from the Fred Hutchinson Cancer Research Center Antibody Development Group, Seattle, WA, U.S.A.) at a dilution of 1:200; an anti-gp130 antibody (to denote the Golgi apparatus) (gp130, Stressgen, Ann Arbor, MI, U.S.A.) at a dilution of 1:250; an anti-PDI (protein disulfide isomerase) antibody (to denote the endoplasmic reticulum) (Stressgen) at a dilution of 1:500; and an anti-E-cadherin [Zymed (Invitrogen), Carlsbad, CA, U.S.A.; 18-0223,], anti-claudin-1 [Zymed (Invitrogen); 71-7800] and anti-occludin [Zymed (Invitrogen); 71-1500] antibodies to view proteins involved in tight junction and cadherin-based adhesion at a dilution of 1:250. For secondary antibody labelling, anti-mouse Alexa Fluor® 555 (Invitrogen; A21425, 1:500) or anti-rabbit Alexa Fluor® 555 (Invitrogen; A21429, 1:500) antibodies were used. DAPI (4′,6-diamidino-2-phenylindole) staining was also performed to visualize nuclei, and immunolocalization imaging was performed using a Zeiss 510 META confocal microscope. Endogenous Cx43 plaques were labelled with the P4G9 anti-Cx43 antibody and immunofluorescent images of equal cell culture area were acquired from both the vector control and the fs230-expressing REKs. An experimenter blinded to the identity of each cell line was asked to count the number of punctate structures present at sites of cell–cell apposition in each image. A gap junction plaque was defined as a punctate immunolabelled structure of a size greater than 0.1 μm. The total number of nuclei (as revealed by DAPI staining) was also counted and the number of punctate structures was divided by the total number of nuclei per image to get the average number of gap junction plaques per cell.

Primary antibodies for Western blot analysis were used as follows: C-terminal Cx43 (Sigma; 1:5000), N-terminal Cx43 (from the Fred Hutchinson Cancer Research Center Antibody Development Group; 1:500), p368 Cx43 (Cell Signaling Technologies; 3511, 1:1000), E-cadherin (Zymed; 18-0223, 1:1000), occludin (Zymed; 71-1500, 1:1000), loricrin (Covance; PRB13-145P, 1:1000), Cx26 (Zymed; 71-0500, 1:1000), CK14 (Neomarkers MS-115-P, 1:1000), claudin-1 (Zymed; 71-7800, 1:1000) and GAPDH (glyceraldehyde-3-phosphate dehydrogenase) (Millipore; MAB374, 1:15,000). Primary antibodies were diluted in 5 % Blotto (Santa Cruz) or 3 % BSA (for p368 Cx43 antibody) and nitrocellulose membranes were incubated with each antibody overnight. Depending on the antibody used, primary antibody detection was performed using

mouse or rabbit IgG IRDye 800 (Rockland Immunochemicals) and mouse or rabbit IgG Alexa Fluor® 680 (Invitrogen) secondary antibodies. Imaging and densitometry were performed using the Odyssey software packaged with the Odyssey IR imaging system (Licor) and data values were plotted using GraphPad Prism v4.0.

Microinjection

REKs were grown to a confluent monolayer and single cells were pressure-microinjected with 5 % Lucifer Yellow (Molecular Probes) [26] using an Eppendorf microinjection system coupled to a Leica inverted epifluorescent microscope. At 1 min after microinjection of Lucifer Yellow dye, the incidence of dye transfer was determined where dye transfer to one or more adjacent cells was deemed positive dye transfer.

Organotypic culture

Culture inserts with a 3.0 μm pore size (BD Biosciences) were coated with a collagen I substrate by mixing 4.25 ml of type I collagen (BD Biosciences) with 0.5 ml of 10× HBSS (Hanks balanced salt solution) with Phenol Red (Sigma), 50 μl of 1.0 M Hepes (Gibco) and 75–100 μl of 1 M NaOH. Collagen was polymerized by incubation at 37 °C for 2 h. The collagen layer was then washed with REK growth medium and REKs were plated at a density of 1.5×10^5 per well in the upper chamber and 2 ml of REK growth medium was placed in the lower chamber. After three days, medium from the upper chamber was removed to expose the confluent REKs to air and to induce differentiation. Cultures were fed daily by replacing the lower chamber medium with 2 ml of fresh REK growth medium. After 2 weeks under differentiation conditions, REKs were processed for histological and Western blot analysis.

Histological analysis

The 2 week organotypic epidermis was fixed with 3.8 % formalin for 5 h. After 5 h, samples were stored at 4 °C in PBS. Tissue processing, embedding, sectioning (5 μm sections) and haemotoxylin and eosin staining was performed as previously described [27].

Acetone-induced injury

Acetone-induced injury was performed as previously described [28]. After 1 week under differentiation conditions, organotypic epidermal cultures were left untreated or treated with 0.5 ml of 100 % acetone for 30 s. Acetone was then washed off and the cultures were placed back in the incubator. Acetone treatment was repeated following 3 days of recovery. At 4 days after the organotypic cultures were allowed to respond to the acetone insult, they were processed for histological analysis.

Scrape-loaded dye-transfer assay

As previously describe in Lai et al. [5], monolayer cultures of REKs were washed once with HBSS and a scrape was made down the centre of each culture plate using a 1 ml pipette tip. Wells were washed once with HBSS and 1.5 mg/ml sulforhodamine B diluted in HBSS was added to the scraped monolayer. After 10 min on ice, cultures were rinsed with PBS and evaluated under a fluorescence microscope. As a control, 2 mg/ml rhodamine-dextran, which cannot pass though gap junctions, was used in a separate set of wells to control for fluorescence uptake due to cell death. Since the specific fluorescence generated from GFP-tagged Cx43 and mutant variants was high, this prevented the use a dye which fluoresces with the same emission as GFP. The area of fluorescence in both groups were outlined and calculated using ImageJ and the area of dye transfer in the rhodamine-dextran group was subtracted from the area of dye transfer in the sulforhodamine group and graphed.

Transepithelial resistance

Transepithelial resistance measurements were taken as reported previously [29]. Briefly, 1.5×10^4 REKs were seeded on to a 3.0-μm pore transwell insert (BD Biosciences). After 24 h, a Millicel-ERS voltmeter (Millipore) was used to measure resistance in ohms. Measurements were taken for five consecutive days and the measurements from days 2 to 4 were averaged and graphed.

Statistics

All statistical tests were performed and graphed using GraphPad Prism v4.0 software. Given the multiple variability factors, assay comparisons between full-length Cx43-expressing REKs and each individual mutant REK cell line created were performed using a t test with a statistical cut-off at $P < 0.05$.

RESULTS

Localization and functional characterization of REKs expressing mutant Cx43

REKs were engineered to express Cx43 or Cx43 mutants associated with ODDD to determine how only a subset of Cx43 mutants can cause skin disease. Two frameshift mutants that have been reported to cause ODDD and palmar plantar hyperkeratosis (fs230 and fs260) [17,18] and one previously characterized Cx43 trafficking mutant [25] were included in the present study. In addition, a mouse G60S mutant [30] that results in a phenotype mimicking the ODDD condition, and further represents a mutation in the first extracellular loop region of Cx43, was also included. The missense human G21R and G138R mutants were selected since these mutants represent amino acid changes in Cx43 motifs within the N-terminal tail and cytoplasmic loop domain respectively. Finally, controls included a REK cell line that expressed the empty viral vector, as well as an REK cell line that expressed full-length Cx43. To assist in Cx43 localization, all Cx43 variants were tagged with GFP at the C-terminal which has been shown to have only minor effects on Cx43 distribution and function [31].

Localization of the Cx43 variants when expressed in REKs revealed that almost all cells were in fact expressing the Cx43 variants (Figure 1). Similar to the full-length Cx43 and endogenous Cx43, the G21R and G138R mutants exhibited a cell surface distribution with abundant gap junction plaques. The G60S mutant, on the other hand, revealed few plaques with the bulk of the mutant retained within intracellular compartments. Both the Δ244* and fs230 mutants exhibited an endoplasmic reticulum-like phenotype with little to no evidence of gap junction plaques. Finally, the fs260 mutant was predominantly expressed in the perinuclear region which we have previously shown to be localized within the endoplasmic reticulum and the Golgi apparatus [4]. To determine which subcellular organelle retained the fs230 mutant, fs230-expressing REKs were immunolabelled for the endoplasmic reticulum resident protein, PDI, and the resident Golgi protein, gp130 (Figure 2A). Only a small fraction of the fs230 mutant was localized to the Golgi apparatus, whereas a large population of the mutant was retained within the

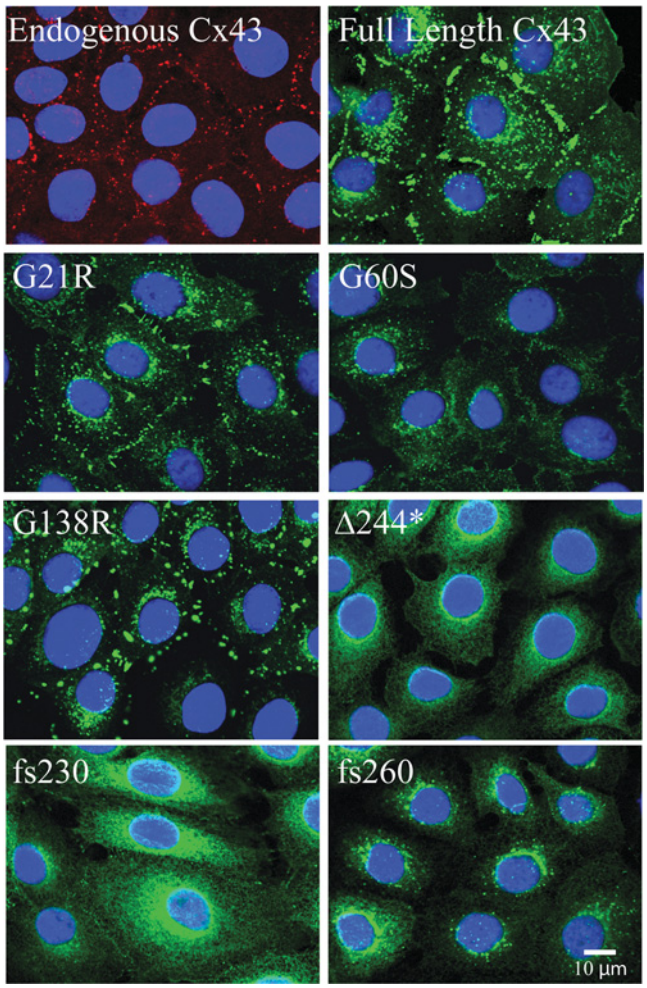

Figure 1 Cx43 mutants display different localization profiles in REKs

REKs were engineered by retroviral infection to stably express GFP-tagged full-length Cx43 (Cx43), two ODDD mutants that cause skin disease (fs230 and fs260), a C-terminal truncation with two additional mutations (Δ244*), as well as three ODDD-linked mutants not associated with skin disease (G21R, G60S and G138R). Full-length Cx43, as well as the G21R and G138R mutants, traffic to the plasma membrane and display large gap junctions, whereas G60S, Δ244*, fs230 and fs260 mutant expression is largely confined to intracellular compartments. Endogenous Cx43 was detected by immunolabelling (red) and nuclei were labelled with DAPI (blue).

endoplasmic reticulum. Since the majority of the ODDD mutants examined thus far have been found to be dominant-negative to endogenous Cx43 [6], the frequency of endogenous Cx43 gap junction plaques were assessed after labelling with an antibody directed to the C-terminal domain of Cx43 that is lacking in the fs230 mutant variant. Compared with cells expressing an empty vector, the number of detectable endogenous Cx43 gap junction plaques was reduced when the fs230 mutant was expressed (Figures 2B and 2C). To determine if the fs230-mutant-expressing REKs could functionally pass Lucifer Yellow dye to their neighbouring cell, Lucifer Yellow dye was injected into REKs expressing the empty vector or the fs230 mutant (Figure 2D and also see Supplementary Figure S1 at http://www.BiochemJ.org/bj/429/bj4290473add.htm). The incidence of dye transfer revealed that 33 % the fs230-mutant-expressing REKs and 100 % of vector control REKs passed dye. This result suggests that the over-expressed fs230 mutant is also dominant–negative to the endogenous Cx43 protein.

To further evaluate the gap junction functional status of each REK cell line created, a dye transfer assay was performed on a wounded monolayer (Figure 3). Scraped monolayers were either treated with a small dye (sulforhodamine B) which can pass through gap junctions (Figure 3A) or, as a negative control, a large dye (rhodamine-dextran) which cannot spread from one cell to another via gap junctions. In each ODDD mutant Cx43-expressing cell line, with the exception of the Δ244*-expressing REKs, there was a significant decrease in the area of dye spread when compared with REKs expressing the full-length Cx43 (Figure 3B). These results suggest that all mutants (except Δ244*) have the capacity to inhibit the function of endogenous Cx43 consistent with previous reports [6,29,32].

Organotypic epidermal differentiation is affected by REKs expressing mutant Cx43

Given that the G21R, G60S, G138R, fs230 and fs260 mutants inhibit overall gap junction coupling in REKs, we sought to determine if this reduced cell coupling state could affect epidermal differentiation (Figure 4). Surprisingly, all REK cell lines possess the ability to differentiate and establish multiple cellular layers (Figure 4A). A basal layer, stratum spinosum, stratum granulosum and stratum corneum developed, suggesting that epidermal formation can proceed with greatly reduced Cx43 gap junction function. Cx43-expressing REKs predominantly developed a tightly packed stratum corneum, whereas in other REK cell lines, spaces were observed within the stratum corneum. In addition, nuclei were often observed in the stratum corneum of fs260-expressing REKs (typically called parakeratosis). The differentiation state was also analysed by measuring the total organotypic architecture and stratum corneum layer thicknesses (corrected for the spaces in the stratum corneum) (Figure 4B). The stratum corneum thickness compared with the entire construct thickness was plotted, and revealed that the G21R, G60S, G138R and fs260 organotypic epidermal cultures all developed a slightly thinner stratum corneum. This suggests that the expression of these ODDD-linked mutants in keratinocytes inhibits the formation of the stratum corneum.

Mutant Cx43 expression reduced the levels of phosphorylated Cx43, Cx26 and loricrin

Since endogenous Cx43 is co-expressed with the Cx43 variants during the differentiation process, the endogenous Cx43 content was examined in organotypic epidermal cultures (Figure 5A). Western blots of organotypic epidermal cultures were performed using an antibody directed to the C-terminus of Cx43 which only detects endogenous Cx43, as well as an antibody directed to the N-terminus of Cx43 suitable for detecting all of the GFP-tagged Cx43 variants. As expected, all REK cell lines expressed the exogenous Cx43 variants to an approximately similar level as ectopic Cx43 with the exception that the Δ244* mutant was under-expressed and the fs230 mutant was over-expressed compared with the other mutants (Figures 5A and 5B). It was notable the over-expression of GFP-tagged Cx43 resulted in an increase in the detectable levels of endogenous Cx43, suggesting that exogenous Cx43 was serving a role in stabilizing the endogenous population of Cx43 (Figures 5A and 5B). Interestingly, the phosphorylated species of endogenous Cx43 (P-Cx43) was reduced (compared with Cx43-over-expressing cells) when the ODDD-associated Cx43 mutants (G21R, G138R, fs230 and fs260) were co-expressed (Figure 5B). Moreover, when Cx43 or the Δ244* mutant was over-expressed, there was an increase in Cx26 levels, and this increase was not evident when any other ODDD-linked mutant was over-expressed (Figure 5C).

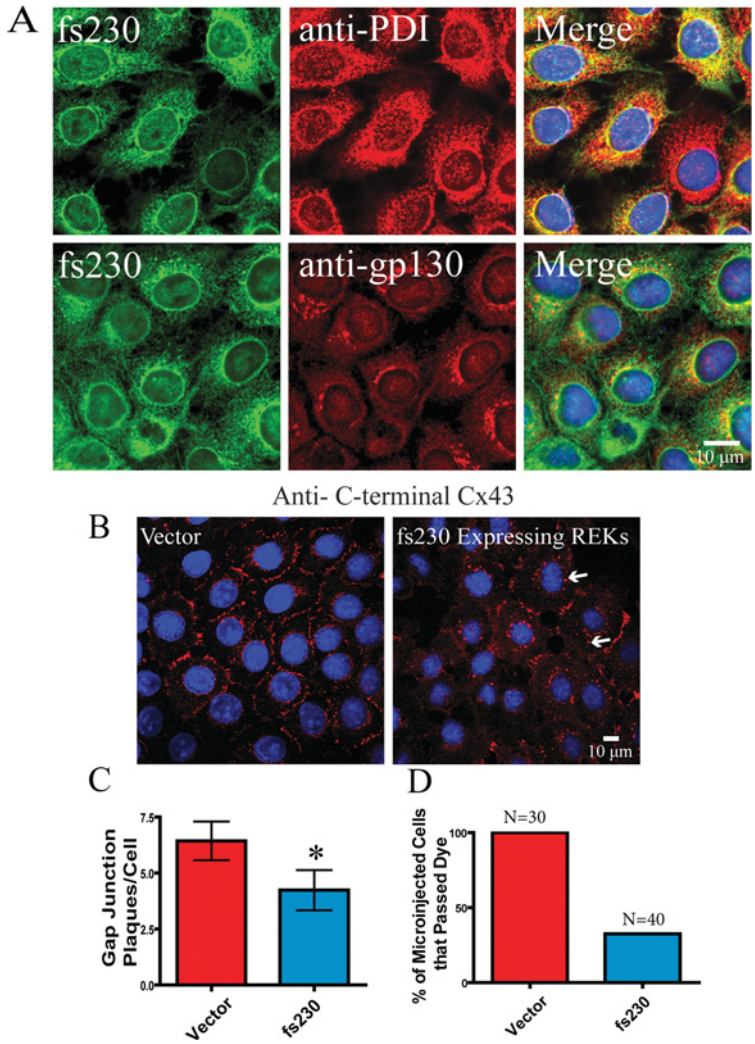

Figure 2 The fs230 mutant is predominantly localized within the endoplasmic reticulum and reduces the number of endogenous gap junctions and the extent of GJIC

(**A**) fs230-expressing REKs were labelled with antibodies specific for PDI (endoplasmic reticulum-resident protein) or gp130 (Golgi marker). The bulk of fs230 co-localized primarily with PDI. Nuclei were stained with DAPI (blue). (**B**) Both vector control and fs230-expressing REKs were immunolabelled with a C-terminal specific anti-Cx43 antibody that detected only endogenous Cx43. Arrows indicate plaque formation. (**C**) fs230-expressing REKs exhibited a 34 % decrease in endogenous Cx43 plaque formation when compared with vector control REKs. (**D**) Lucifer Yellow dye was microinjected into both vector control and fs230-expressing REKs. All vector control REKs passed Lucifer Yellow dye, whereas only 33 % of fs230-expressing REKs passed dye to neighbouring cells. $^{*}P < 0.05$.

Of all the mutants tested, only the fs260 mutant reduced the P_0 state of endogenous Cx43 when compared with ectopic Cx43, and this mutant was the only one to significantly inhibit the state of organotypic differentiation as assessed by a reduction in a key molecular marker of differentiation, loricrin (Figure 5D). Finally, comparable with the total reduction in endogenous Cx43 levels, the fs260 mutant was found to reduce the level of the Cx43 species phosphorylated on Ser^{368} as detected by an anti-p368 Cx43 phospho-specific antibody (see Supplementary Figure S2 at http://www.BiochemJ.org/bj/429/bj4290473add.htm).

Reduced barrier function in REKs expressing G60S, G138R and fs260 Cx43 mutants

Since the epidermal barrier is important for proper epidermal function, and Cx43 has been found to cross-talk with other junctional complexes [33,34], we assessed if mutant Cx43-expressing REKs can disrupt the transepithelial resistance (Figure 6). Collectively, REKs which expressed the G60S, G138R and fs260 ODDD-linked mutants exhibited lower transepithelial resistance when compared with ectopic Cx43-expressing REKs (Figure 6A). However, this reduction in transepithelial resistance was not due to expression level (Figures 6C and 6D) or subcellular localization changes in occludin or claudin-1 or a change in the cell adhesion protein, E-cadherin (Figure 6B). In addition, reduced transepithelial resistance was not due to differences in cell death as revealed through the use of the MultiTox cell death assay (results not shown).

Organotypic epidermis expressing fs260 increased the vital layer thickness after acetone-induced injury

We showed that organotypic cultures expressing the fs260 mutant developed a thinner stratum corneum thickness and exhibited

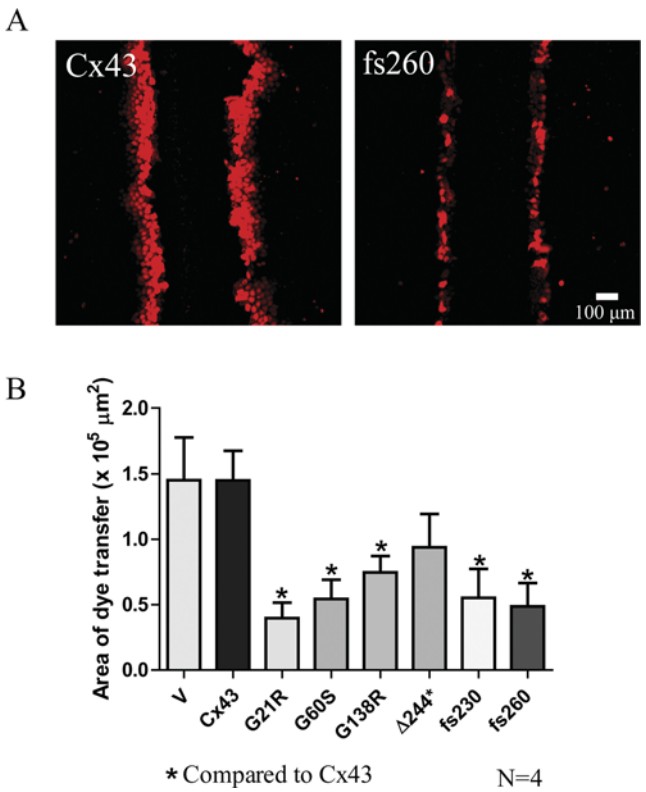

Figure 3 Cx43 mutants reduce dye transfer in REKs

(**A**) To assess the ability of REKs to transfer dye to neighbouring cells, a scrape assay was performed using a gap junction permeable dye, sulforhodamine. (**B**) With the exception of Δ244*, there was a significant reduction in dye spread in mutant expressing REKs compared with Cx43-overexpressing REKs. V, empty vector. $*P < 0.05$.

parakeratosis. In addition, REKs expressing the fs260 mutant lowered the endogenous expression of Cx43, Cx26 and loricrin, and lowered the transepithelial resistance. Given these changes, REKs expressing this mutant may develop an aberrant epidermal barrier. To determine if the expression of mutant Cx43 in organotypic cultures can affect the response of the epidermal cultures to injury, an acetone-induced injury and recovery assay was performed (Figure 7). The stratum corneum in the full-length Cx43-expressing REKs remained compact after acetone treatment, whereas nuclei were enriched in the stratum corneum of fs260-expressing organotypic cultures (Figure 7A). Since acetone treatment has been shown to induce a proliferative response [28], vital layer thickness measurements were compared between untreated and acetone-treated organotypic epidermal cultures (Figure 7B). Altough no differences were observed in the vital layer thickness in full-length Cx43-expressing cultures, the fs260-expressing cultures formed a significantly larger vital layer thickness after treatment with acetone.

DISCUSSION

Mutations in the gene encoding Cx43 have been conclusively linked to ODDD. Although there are currently 62 mutations that have been reported to cause ODDD [12], only the fs230 and fs260 Cx43 mutants have been reported to result in an additional skin disease phenotype [17,18]. In the case of the fs230 mutant, this is not always the case, as a patient recently shown to be harbouring this mutant exhibited no evidence of skin disease [19]. The skin disease associated with these two mutants has been classified as palmar planter hyperkeratosis and the molecular etiology by which Cx43 mutations can cause skin disease remains unknown. To determine how select mutants can cause skin disease, various Cx43 constructs were expressed in REKs and assessed for their cellular localization, functional status, organotypic differentiation potential, transepithelial resistance, effect on endogenously expressed connexins and finally response to chemical injury. In all assays performed, only the fs260-mutant-expressing REKs consistently exhibit epidermal defects, and we propose that the additive effects of these defects ultimately lead to palmar plantar hyperkeratosis.

Subcellular localization may reflect the potency of ODDD mutants

The fs230 and fs260 mutants are similar in that they result in C-terminal tail truncations but they differ dramatically in the extra non-connexin amino acid length. The fs230 mutant only has six extra amino acids [18], whereas the fs260 mutant possesses an additional 46 amino acids [17]. Although both of these mutants have been shown to be linked to palmar plantar hyperkeratosis, the fs230 mutant does not consistently cause this skin disease in all patients [19], which may be mechanistically linked to their primary subcellular residence. Immunofluorescent localization studies revealed that the fs230 mutant primarily resides in the endoplasmic reticulum. Although the fs260 mutant is also found in the endoplasmic reticulum when it is expressed in REKs [4], a significant population escapes this compartment and reaches the Golgi apparatus [4]. The importance of this finding is rooted in the fact that Cx43 oligomerization does not occur in the endoplasmic reticulum, possibly because of its interaction with ERp19 [35], with final oligomerization being delayed until the Golgi apparatus [36]. Thus the bolus of the fs260 mutant in the Golgi apparatus would have an increased opportunity to oligomerize and inactivate co-expressed wild-type Cx43 by both preventing further transport to the cell surface and inhibiting channel function. Of all the frameshift and missense Cx43 mutants examined to date, this characteristic of accumulating in the Golgi apparatus is unique to fs260. Thus our results suggest that the fs230 mutant is not as potent in causing skin disease and this aetiology may not manifest in all patients harbouring this mutation, as seems to be the case.

fs260-expressing REKs develop epidermal defects not observed by other ODDD mutants

A major advantage in using the REK cell line is the ability to model epidermal differentiation in culture. Surprisingly, all cell lines examined retain the ability to differentiate and form epidermal layers as found in thin skin. It was observed that the full-length Cx43-expressing REKs did, however, form a very compact stratum corneum. Since proper calcium signalling in the upper stratum granulosum has been shown to facilitate the release of keratohyalin granules, cleave stratum corneum precursor proteins (profillagrin) and activate transglutaminases to cross-link proteins of the stratum corneum (loricrin) [37], over-expression of functional Cx43 may enhance calcium signalling and facilitate the formation of this phenotype. Morphological evaluation of the organotypic epidermal cultures revealed that the stratum corneum layer thickness was largest in the REK cell lines which expressed Cx43 variants (Cx43 and Δ244*) that both maintained their dye-transfer ability and the expression of the most phosphorylated Cx43 species. Since cells expressing both the Cx43 and Δ244* constructs developed a larger stratum corneum, we suggest that functional Cx43 levels can enhance

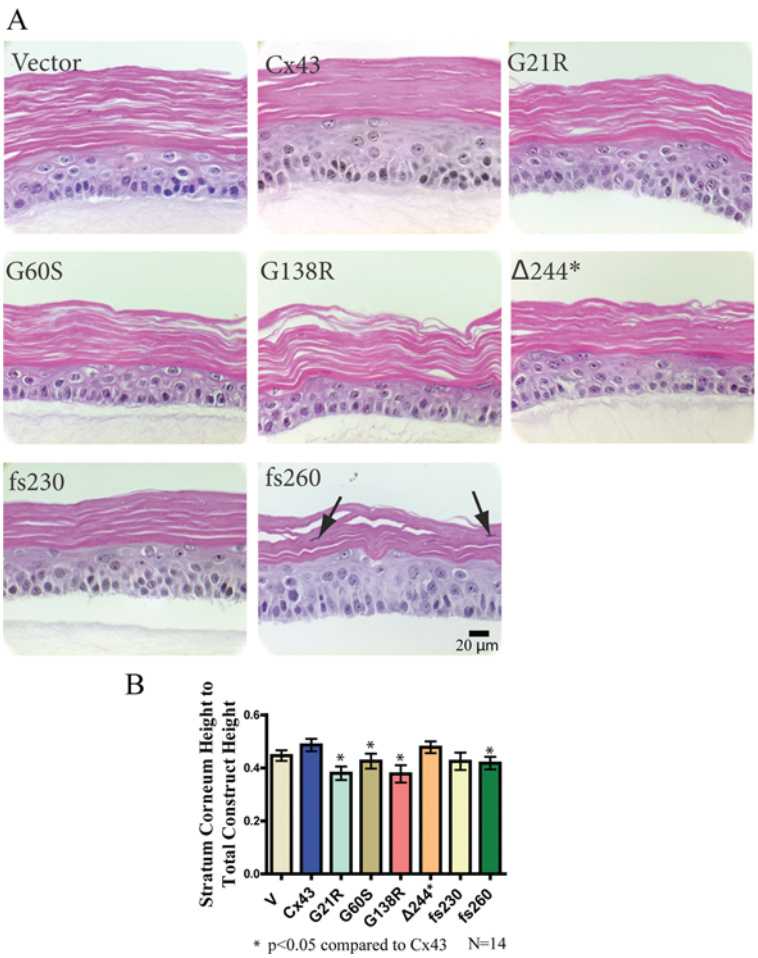

Figure 4 Cx43 mutant-expressing REKs differentiate into organotypic epidermis

REKs were plated on to collagen type I-coated well inserts and the medium from the upper chamber was removed to allow REKs to differentiate and stratify. (**A**) After two weeks of organotypic differentiation, all mutant expressing Cx43 REK cell lines differentiated. To determine the extent of organotypic differentiation, histological sections of each organotypic culture were stained with haematoxylin and eosin, imaged, and the upper stratum corneum and lower vital layer thicknesses were measured. (**B**) When comparing the stratum corneum height with total epidermal height, there was a significant decrease found in the G21R-, G60S-, G138R- and fs260-expressing cultures when compared with organotypic cultures derived from Cx43 expressing REKs. In addition, parakeratosis was observed in the fs260-expressing cultures (arrows). $^{*}P < 0.05$.

the differentiation state of the epidermis. This is also supported by evidence that Cx43 is enhanced during restratification of the epidermis during development and after wound healing [38–41].

Given that a feature of hyperkeratosis is an enlarged stratum corneum, the observed decrease in the stratum corneum thickness in the fs260-expressing organotypic cultures was not expected. Since palmar plantar hyperkeratosis is only seen in a thick skin environment, our organotypic epidermal cultures may model a thin skin environment and not fully mimic the disease state found in thick skin. In addition, the relatively short time period used to establish organotypic epidermal cultures may only assess how mutant Cx43 affects the development of the epidermis and not represent the resulting steady state and maintenance after differentiation. Over time, keratinocytes expressing ODDD-associated mutants may undergo unnecessary proliferative and regenerative events to result in an enlarged stratum corneum. The fs260-expressing organoytpic epidermal cultures did, however, reveal nuclei present in the stratum corneum. However, this feature is often observed in hyperkeratosis [42] and suggests that the fs260-expressing keratinocytes may have a higher propensity to develop hyperkeratosis *in vivo*.

Cx26 cross-talk with Cx43 mutants

To biochemically assess the differentiation state of these organotypic cultures, Cx26, loricrin and CK14 were evaluated using Western blot analysis. Cx26 is normally expressed in the stratum granulosum layer under terminal differentiation conditions and this expression was found to be lower in the ODDD mutant Cx43 expressing organotypic cultures as compared with REKs over-expressing full-length Cx43. Mutant Cx26 has previously been shown to be transdominant to Cx43 [23] and thus mutant Cx43 may also be transdominant to Cx26. Since Cx26 mutants are strongly correlated with skin disease (hyperkeratosis) [43–45], Cx43 mutants which reduce Cx26 levels may also contribute mechanistically to any resulting skin disease phenotype and also wound repair [46].

Decreased levels of Cx43 may lead to epidermal barrier defects

Truncation of the C-terminal tail of Cx43 has previously been shown to disrupt the epidermal barrier in mice [47]. To determine if the epidermal barrier function could also

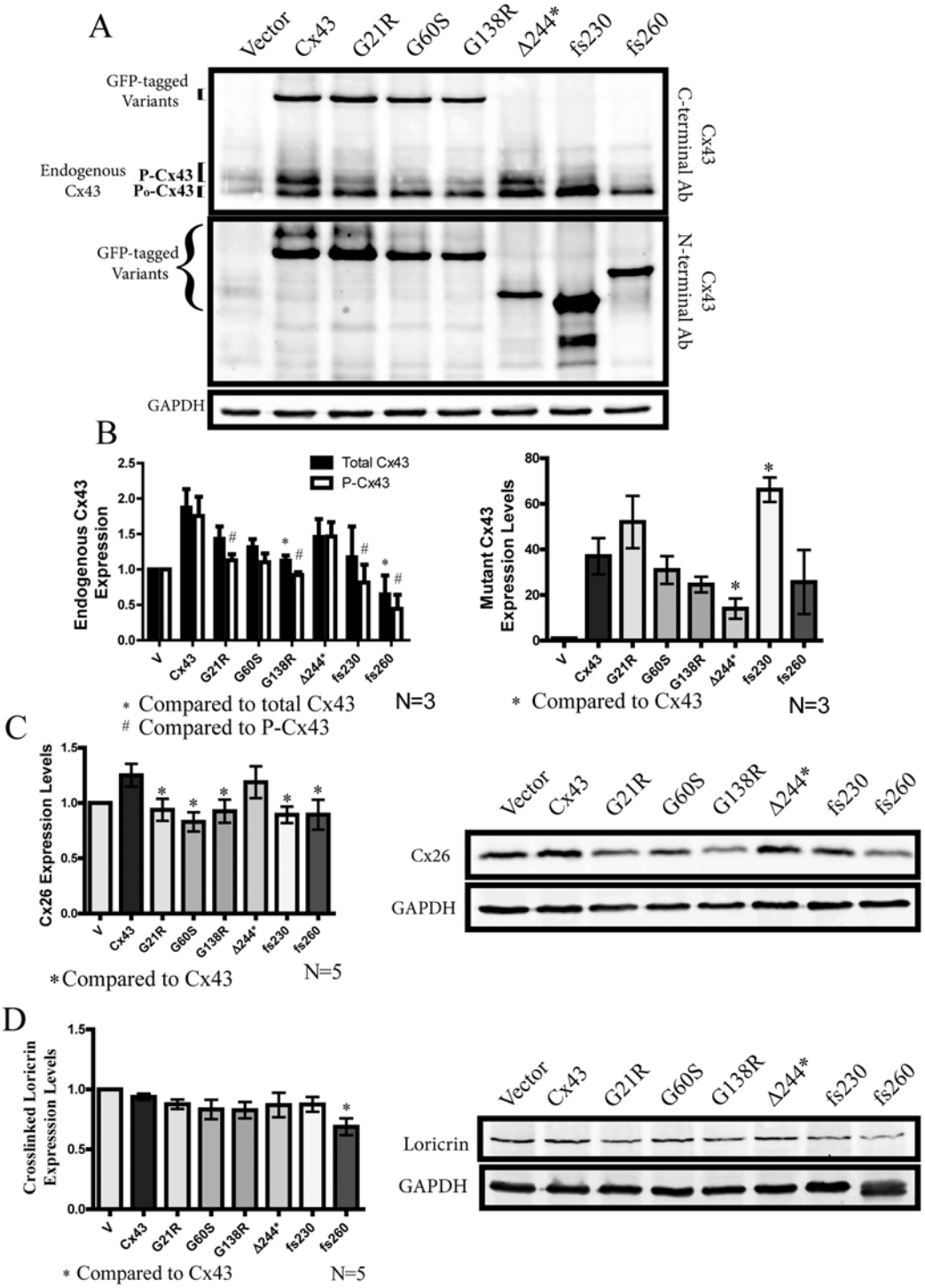

Figure 5 Assessment of endogenous and mutant Cx43, Cx26 and loricrin protein expression in organotypic epidermis

Western blots were performed on REK cells lines after 2 weeks of differentiation. (**A**) Anti-Cx43 N-terminal-specific antibody (Ab) was used to detect GFP-tagged mutant Cx43 variants, whereas an anti-Cx43 C-terminal-specific antibody was used to detect endogenous Cx43 expression. (**B**) The G138R- and fs260-expressing REKs had significantly lower total endogenous Cx43 levels when compared with full-length Cx43 REKs. ODDD mutants also reduced the highly phosphorylated species of endogenous Cx43. Densitometry analysis of GFP-tagged Cx43 variants also revealed a significant decrease in the expression of the Δ244* mutant, whereas the expression of the fs230 mutant was signficantly elevated. In addition, Western blot analysis of Cx26 (**C**) revealed that all ODDD Cx43 mutants reduced the levels of Cx26 compared with cells expressing full-length Cx43, whereas loricrin (**D**) was only reduced in fs260-expressing REKs. $^{*}P < 0.05$ and $^{\#}P < 0.05$.

be affected in REKs expressing mutant Cx43, transepithelial resistance measurements and an acetone-induced injury assay was performed on organotypic cultures derived from each REK cell line created. Although transepithelial resistance measurements assess the paracellular barrier formed by tight junctions, nevertheless, the introduction of Cx43 mutants lowered the transepithelial resistance values but had no effect on the levels or localization of claudin-1 or occludin, suggesting that the cross-talk

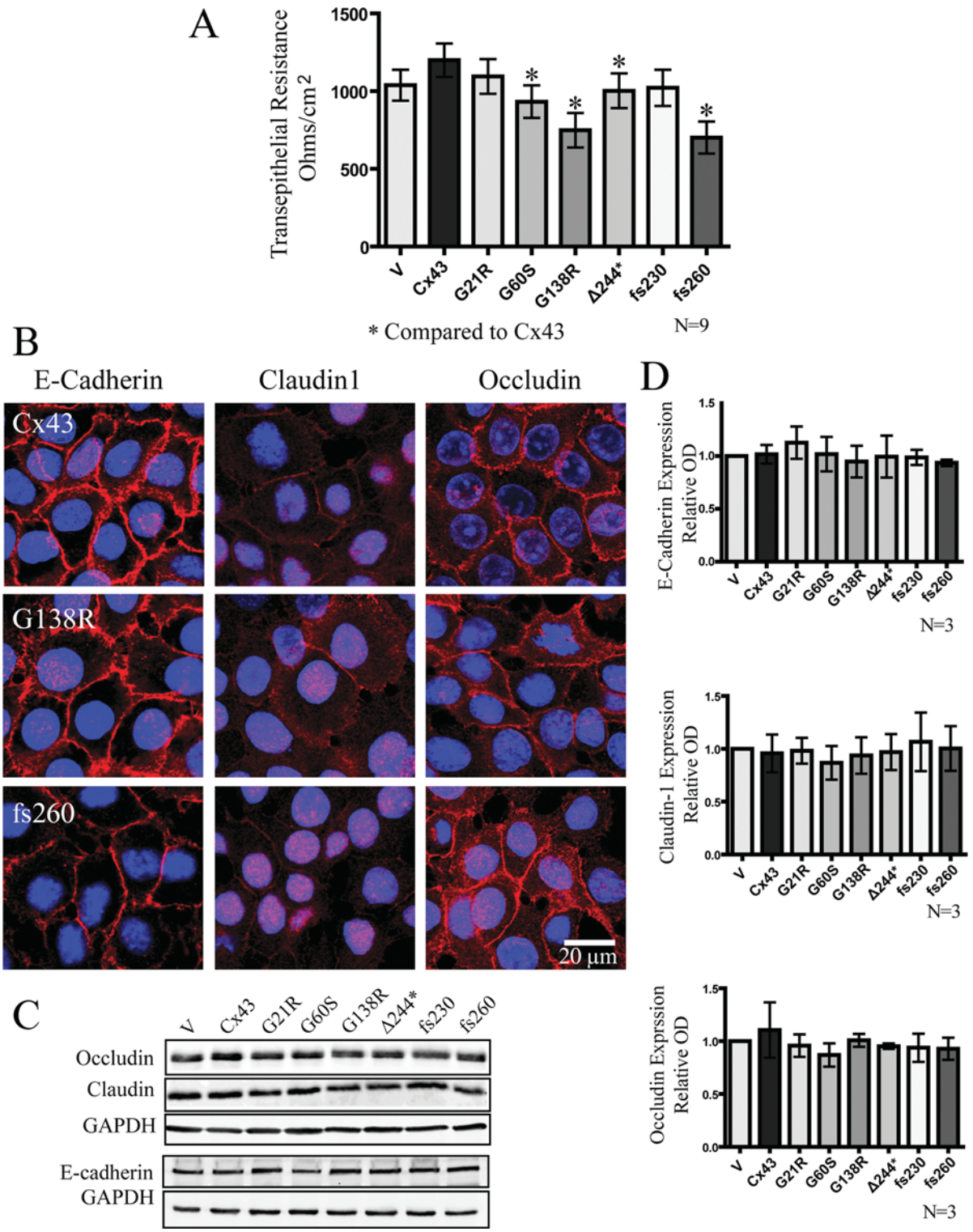

Figure 6 Cx43 mutant-expressing REKs exhibited reduced transepithelial resistance when compared with Cx43 overexpressing REKs in the absence of changes in the expression or localization of junctional proteins

(**A**) Transepithelial resistance measurements of confluent monolayer cultures were taken daily for 5 days and the resistance from days 2–4 were averaged and plotted. (**B**) E-cadherin, claudin1 and occludin were localized by immunofluorescent labelling in REKs overexpressing GFP-tagged Cx43, G138R or fs260. Western blot analysis did not reveal any changes in the expression of occludin, E-cadherin or claudin-1 (**C** and **D**). *$P < 0.05$. Nuclei were labelled with DAPI (blue). GAPDH, glyceraldehyde-3-phosphate dehydrogenase

between the gap junction status and tight junctions may be at the level of junction assembly and not at gene expression [48]. Given that the G60S, G138R and fs260 mutants all moderately reduce transepithelial resistance, palmar plantar hyperkeratosis cannot be rooted solely to this finding. The fs260 mutant, however, did cause the greatest decrease in transepithelial resistance, and since

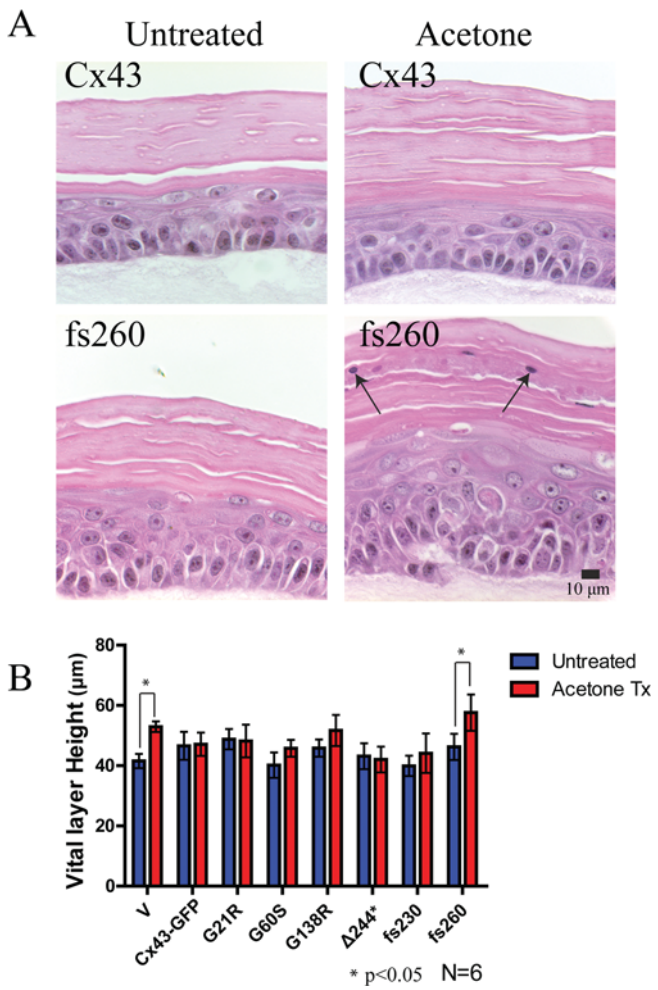

Figure 7 Acetone treatment increased the vital layer thickness in fs260-expressing organotypic cultures

(**A**) Organotypic cultures of REKs expressing endogenous Cx43 or overexpressing Cx43 or Cx43 mutants were left untreated or treated with acetone. Note that in fs260-expressing REK epidermis, there were nuclei present in the stratum corneum (arrows). (**B**) Vital layer measurements of all REK cell lines either untreated or treated with acetone revealed a significant increase in the vital layer thickness in both the vector and fs260-expressing REKs when compared with full-length Cx43 expressing organotypic cultures. $^{*}P < 0.05$.

this mutant reduces the levels of phosphorylated Cx43, which is typically reflective of assembled gap junctions, other junctional complexes may be disrupted leaving the epidermis more prone to dysregulation when placed under stress. This in turn may lead to a proliferative response, an increase in epidermal thickness and hyperkeratosis. Topical application of retinoic acid has been used to treat hyperkeratosis [49] and retinoic acid treatment has been shown to upregulate Cx43 expression [50,51]. Thus the upregulation of Cx43 may promote and stabilize the formation of junctional complexes and further maintain keratinocytes in a non-proliferative state.

To further determine if keratinocytes expressing mutant Cx43 have a normal epidermal barrier, acetone was administered to organotypic cultures and histological analysis was performed after 1 week of injury. Acetone treatment has previously been shown to induce a proliferative response in organotypic cultures [28]. Organotypic cultures expressing full-length Cx43 formed a compact epidermal barrier and no increase in the vital layer was seen as found in cultures that lacked Cx43 overexpression. However, a significant increase in vital layer thickness was observed in fs260-expressing organotypic cultures. Collectively, these results suggest that Cx43, as well as most of the mutant variants of Cx43, but not fs260, can protect against acetone-induced injury.

Although all mutations in the gene encoding Cx43 lead to ODDD, some mutations are clearly more potent, leading to skin abnormalities. Typically, domain-specific Cx43 mutants all cause one or more measureable defects in processes related to epidermal differentiation. However, the fs260 mutant consistently caused quantifiable defects in REKs. In particular, organotypic cultures grown from cells expressing the fs260 mutant developed a thinner stratum corneum with nuclei often present and an enlarged vital layer when exposed to acetone. We proposed that the additive effects of these changes ultimately cause the skin disease phenotype observed in ODDD patients that express this mutant. Thus our findings demonstrate how one Cx43 mutant can cause increased disease burden over and above that caused by other Cx43 mutants.

AUTHOR CONTRIBUTION

Jared Churko performed the majority of the experiments, prepared the Figures, performed the data analysis and drafted the manuscript. Stephanie Langlois contributed by editing the manuscript and teaching Jared Churko some of the methods used in the study. Xingue Pan contributed by performing the gap junction plaque counts and measuring the thickness of the organotypic layers. Qing Shao contributed by designing many of the Cx43 mutants used in this study. Dale Laird is the principal investigator leading this study and edited the manuscript.

FUNDING

This work was funded by a Canadian Institutes of Health Research operating grant [grant number MOP 74637] (to D.W.L.) and a Natural Sciences and Engineering Research Council of Canada studentship grant (to J.M.C.).

REFERENCES

1 Beyer, E. C., Paul, D. L. and Goodenough, D. A. (1987) Connexin43: a protein from rat heart homologous to a gap junction protein from liver. J. Cell Biol. **105**, 2621–2629
2 Vanslyke, J. K., Naus, C. C. and Musil, L. S. (2009) Conformational maturation and post-ER multisubunit assembly of gap junction proteins. Mol. Biol. Cell **20**, 2451–2463
3 Goodenough, D. A., Goliger, J. A. and Paul, D. L. (1996) Connexins, connexons, and intercellular communication. Annu. Rev. Biochem. **65**, 475–502
4 Gong, X. Q., Shao, Q., Lounsbury, C. S., Bai, D. and Laird, D. W. (2006) Functional characterization of a GJA1 frameshift mutation causing oculodentodigital dysplasia and palmoplantar keratoderma. J. Biol. Chem. **281**, 31801–31811
5 Lai, A., Le, D. N., Paznekas, W. A., Gifford, W. D., Jabs, E. W. and Charles, A. C. (2006) Oculodentodigital dysplasia connexin43 mutations result in non-functional connexin hemichannels and gap junctions in C6 glioma cells. J. Cell Sci. **119**, 532–541
6 McLachlan, E., Manias, J. L., Gong, X. Q., Lounsbury, C. S., Shao, Q., Bernier, S. M., Bai, D. and Laird, D. W. (2005) Functional characterization of oculodentodigital dysplasia-associated Cx43 mutants. Cell Commun. Adhes. **12**, 279–292
7 Richard, G. (2005) Connexin disorders of the skin. Clin. Dermatol. **23**, 23–32
8 White, T. W., Deans, M. R., O'Brien, J., Al-Ubaidi, M. R., Goodenough, D. A., Ripps, H. and Bruzzone, R. (1999) Functional characteristics of skate connexin35, a member of the gamma subfamily of connexins expressed in the vertebrate retina. Eur. J. Neurosci. **11**, 1883–1890
9 Petit, C. (2006) From deafness genes to hearing mechanisms: harmony and counterpoint. Trends Mol. Med. **12**, 57–64
10 Gutstein, D. E., Morley, G. E., Tamaddon, H., Vaidya, D., Schneider, M. D., Chen, J., Chien, K. R., Stuhlmann, H. and Fishman, G. I. (2001) Conduction slowing and sudden arrhythmic death in mice with cardiac-restricted inactivation of connexin43. Circ. Res. **88**, 333–339
11 Scherer, S. S., Bone, L. J., Deschenes, S. M., Abel, A., Balice-Gordon, R. J. and Fischbeck, K. H. (1999) The role of the gap junction protein connexin32 in the pathogenesis of X-linked Charcot–Marie–Tooth disease. Novartis Found. Symp. **219**, 175–185

12 Paznekas, W. A., Karczeski, B., Vermeer, S., Lowry, R. B., Delatycki, M., Laurence, F., Koivisto, P. A., Van Maldergem, L., Boyadjiev, S. A., Bodurtha, J. N. and Jabs, E. W. (2009) GJA1 mutations, variants, and connexin 43 dysfunction as it relates to the oculodentodigital dysplasia phenotype. Hum. Mutat. **30**, 724–733

13 Gillespie, F. D. (1964) A hereditary syndrome: "dysplasia oculodentodigitalis". Arch. Ophthalmol. **71**, 187–192

14 Gutmann, D. H., Zackai, E. H., Donald-McGinn, D. M., Fischbeck, K. H. and Kamholz, J. (1991) Oculodentodigital dysplasia syndrome associated with abnormal cerebral white matter. Am. J. Med. Genet. **41**, 18–20

15 Kelly, S. C., Ratajczak, P., Keller, M., Purcell, S. M., Griffin, T. and Richard, G. (2006) A novel GJA 1 mutation in oculo-dento-digital dysplasia with curly hair and hyperkeratosis. Eur. J. Dermatol. **16**, 241–245

16 Kjaer, K. W., Hansen, L., Eiberg, H., Leicht, P., Opitz, J. M. and Tommerup, N. (2004) Novel connexin 43 (GJA1) mutation causes oculo-dento-digital dysplasia with curly hair. Am. J. Med. Genet. A **127A**, 152–157

17 van Steensel, M. A., Spruijt, L., van der Burgt, I., Bladergroen, R. S., Vermeer, M., Steijlen, P. M. and van Geel, M. (2005) A 2-bp deletion in the GJA1 gene is associated with oculo-dento-digital dysplasia with palmoplantar keratoderma. Am. J. Med. Genet. A. **132A**, 171–174

18 Vreeburg, M., de Zwart-Storm, E. A., Schouten, M. I., Nellen, R. G., Marcus-Soekarman, D., Devies, M., van Geel, M. and van Steensel, M. A. (2007) Skin changes in oculo-dento-digital dysplasia are correlated with C-terminal truncations of connexin 43. Am. J. Med. Genet. A. **143**, 360–363

19 Alao, M. J., Bonneau, D., Holder-Espinasse, M., Goizet, C., Manouvrier-Hanu, S., Mezel, A., Petit, F., Subtil, D., Magdelaine, C. and Lacombe, D. (2010) Oculo-dento-digital dysplasia: lack of genotype-phenotype correlation for GJA1 mutations and usefulness of neuro-imaging. Eur. J. Med. Genet. **53**, 19–22

20 Kimonis, V., DiGiovanna, J. J., Yang, J. M., Doyle, S. Z., Bale, S. J. and Compton, J. G. (1994) A mutation in the V1 end domain of keratin 1 in non-epidermolytic palmar-plantar keratoderma. J. Invest. Dermatol. **103**, 764–769

21 de Zwart-Storm, E. A., Hamm, H., Stoevesandt, J., Steijlen, P. M., Martin, P. E., van Geel, M. and van Steensel, M. A. (2008) A novel missense mutation in GJB2 disturbs gap junction protein transport and causes focal palmoplantar keratoderma with deafness. J. Med. Genet. **45**, 161–166

22 Bragg, J., Rizzo, C. and Mengden, S. (2008) Striate palmoplantar keratoderma (Brunauer–Fohs–Siemens syndrome). Dermatol. Online J. **14**, 26

23 Rouan, F., White, T. W., Brown, N., Taylor, A. M., Lucke, T. W., Paul, D. L., Munro, C. S., Uitto, J., Hodgins, M. B. and Richard, G. (2001) *trans*-dominant inhibition of connexin-43 by mutant connexin-26: implications for dominant connexin disorders affecting epidermal differentiation. J. Cell Sci. **114**, 2105–2113

24 Baden, H. P. and Kubilus, J. (1983) The growth and differentiation of cultured newborn rat keratinocytes. J. Invest. Dermatol. **80**, 124–130

25 Simek, J., Churko, J., Shao, Q. and Laird, D. W. (2009) Cx43 has distinct mobility within plasma-membrane domains, indicative of progressive formation of gap-junction plaques. J. Cell Sci. **122**, 554–562

26 Thomas, T., Telford, D. and Laird, D. W. (2004) Functional domain mapping and selective trans-dominant effects exhibited by Cx26 disease-causing mutations. J. Biol. Chem. **279**, 19157–19168

27 Langlois, S., Churko, J. M. and Laird, D. W. (2009) Optical and biochemical dissection of connexin and disease-linked connexin mutants in 3D organotypic epidermis. In Epidermal Cells (Turksen, K., ed.), pp. 313–335, Springer Protocols, Berlin

28 Ajani, G., Sato, N., Mack, J. A. and Maytin, E. V. (2007) Cellular responses to disruption of the permeability barrier in a three-dimensional organotypic epidermal model. Exp. Cell Res. **313**, 3005–3015

29 Langlois, S., Maher, A. C., Manias, J. L., Shao, Q., Kidder, G. M. and Laird, D. W. (2007) Connexin levels regulate keratinocyte differentiation in the epidermis. J. Biol. Chem. **282**, 30171–30180

30 Flenniken, A. M., Osborne, L. R., Anderson, N., Ciliberti, N., Fleming, C., Gittens, J. E., Gong, X. Q., Kelsey, L. B., Lounsbury, C., Moreno, L. et al. (2005) A Gja1 missense mutation in a mouse model of oculodentodigital dysplasia. Development **132**, 4375–4386

31 Laird, D. W., Jordan, K., Thomas, T., Qin, H., Fistouris, P. and Shao, Q. (2001) Comparative analysis and application of fluorescent protein-tagged connexins. Microsc. Res. Tech. **52**, 263–272

32 Gong, X. Q., Shao, Q., Langlois, S., Bai, D. and Laird, D. W. (2007) Differential potency of dominant negative connexin43 mutants in oculodentodigital dysplasia. J. Biol. Chem. **282**, 19190–19202

33 Nagasawa, K., Chiba, H., Fujita, H., Kojima, T., Saito, T., Endo, T. and Sawada, N. (2006) Possible involvement of gap junctions in the barrier function of tight junctions of brain and lung endothelial cells. J. Cell Physiol. **208**, 123–132

34 Li, M. W., Mruk, D. D., Lee, W. M. and Cheng, C. Y. (2009) Connexin 43 and plakophilin-2 as a protein complex that regulates blood-testis barrier dynamics. Proc. Natl. Acad. Sci. U.S.A. **106**, 10213–10218

35 Das, S., Smith, T. D., Sarma, J. D., Ritzenthaler, J. D., Maza, J., Kaplan, B. E., Cunningham, L. A., Suaud, L., Hubbard, M. J., Rubenstein, R. C. and Koval, M. (2009) ERp29 restricts Connexin43 oligomerization in the endoplasmic reticulum. Mol. Biol. Cell **20**, 2593–2604

36 Musil, L. S. and Goodenough, D. A. (1993) Multisubunit assembly of an integral plasma membrane channel protein, gap junction connexin43, occurs after exit from the ER. Cell **74**, 1065–1077

37 Kimyai-Asadi, A., Kotcher, L. B. and Jih, M. H. (2002) The molecular basis of hereditary palmoplantar keratodermas. J. Am. Acad. Dermatol. **47**, 327–343

38 Choudhry, R., Pitts, J. D. and Hodgins, M. B. (1997) Changing patterns of gap junctional intercellular communication and connexin distribution in mouse epidermis and hair follicles during embryonic development. Dev. Dyn. **210**, 417–430

39 Goliger, J. A. and Paul, D. L. (1994) Expression of gap junction proteins Cx26, Cx31.1, Cx37, and Cx43 in developing and mature rat epidermis. Dev. Dyn. **200**, 1–13

40 Richards, T. S., Dunn, C. A., Carter, W. G., Usui, M. L., Olerud, J. E. and Lampe, P. D. (2004) Protein kinase C spatially and temporally regulates gap junctional communication during human wound repair via phosphorylation of connexin43 on serine368. J. Cell Biol. **167**, 555–562

41 Kretz, M., Euwens, C., Hombach, S., Eckardt, D., Teubner, B., Traub, O., Willecke, K. and Ott, T. (2003) Altered connexin expression and wound healing in the epidermis of connexin-deficient mice. J. Cell Sci. **116**, 3443–3452

42 Chopra, A., Maninder and Gill, S. (1997) Histopathological study of hyperkeratosis of palms and soles. Indian J. Dermatol. Venereol. Leprol. **63**, 85–88

43 Iossa, S., Chinetti, V., Auletta, G., Laria, C., De Luca, M., Rienzo, M., Giannini, P., Delfino, M., Ciccodicola, A., Marciano, E. and Franze, A. (2009) New evidence for the correlation of the p.G130V mutation in the GJB2 gene and syndromic hearing loss with palmoplantar keratoderma. Am. J. Med. Genet. A. **149A**, 685–688

44 Maestrini, E., Korge, B. P., Ocana-Sierra, J., Calzolari, E., Cambiaghi, S., Scudder, P. M., Hovnanian, A., Monaco, A. P. and Munro, C. S. (1999) A missense mutation in connexin26, D66H, causes mutilating keratoderma with sensorineural deafness (Vohwinkel's syndrome) in three unrelated families. Hum. Mol. Genet. **8**, 1237–1243

45 Uyguner, O., Tukel, T., Baykal, C., Eris, H., Emiroglu, M., Hafiz, G., Ghanbari, A., Baserer, N., Yuksel-Apak, M. and Wollnik, B. (2002) The novel R75Q mutation in the GJB2 gene causes autosomal dominant hearing loss and palmoplantar keratoderma in a Turkish family. Clin. Genet. **62**, 306–309

46 Goliger, J. A. and Paul, D. L. (1995) Wounding alters epidermal connexin expression and gap junction-mediated intercellular communication. Mol. Biol. Cell **6**, 1491–1501

47 Maass, K., Ghanem, A., Kim, J. S., Saathoff, M., Urschel, S., Kirfel, G., Grummer, R., Kretz, M., Lewalter, T., Tiemann, K. et al. (2004) Defective epidermal barrier in neonatal mice lacking the C-terminal region of connexin43. Mol. Biol. Cell **15**, 4597–4608

48 de Carvalho, A. D., de Souza, W. and Morgado-Diaz, J. A. (2006) Morphological and molecular alterations at the junctional complex in irradiated human colon adenocarcinoma cells, Caco-2. Int. J. Radiat. Biol. **82**, 658–668

49 Braun-Falco, M. (2009) Hereditary palmoplantar keratodermas. J. Dtsch. Dermatol. Ges. **7**, 971–984

50 Masgrau-Peya, E., Salomon, D., Saurat, J. H. and Meda, P. (1997) *In vivo* modulation of connexins 43 and 26 of human epidermis by topical retinoic acid treatment. J. Histochem. Cytochem. **45**, 1207–1215

51 Guo, H., Acevedo, P., Parsa, F. D. and Bertram, J. S. (1992) Gap-junctional protein connexin 43 is expressed in dermis and epidermis of human skin: differential modulation by retinoids. J. Invest. Dermatol. **99**, 460–467

Received 27 January 2010/19 May 2010; accepted 1 June 2010
Published as BJ Immediate Publication 1 June 2010, doi:10.1042/BJ20100155

Biochem. J. (2010) **429**, 473–483 (Printed in Great Britain) doi:10.1042/BJ20100155

online data

SUPPLEMENTARY ONLINE DATA

The potency of the fs260 connexin43 mutant to impair keratinocyte differentiation is distinct from other disease-linked connexin43 mutants

Jared M. CHURKO, Stephanie LANGLOIS, Xinyue PAN, Qing SHAO and Dale W. LAIRD[1]

Department of Anatomy and Cell Biology, University of Western Ontario, London, Ontario, Canada N6A 5C1

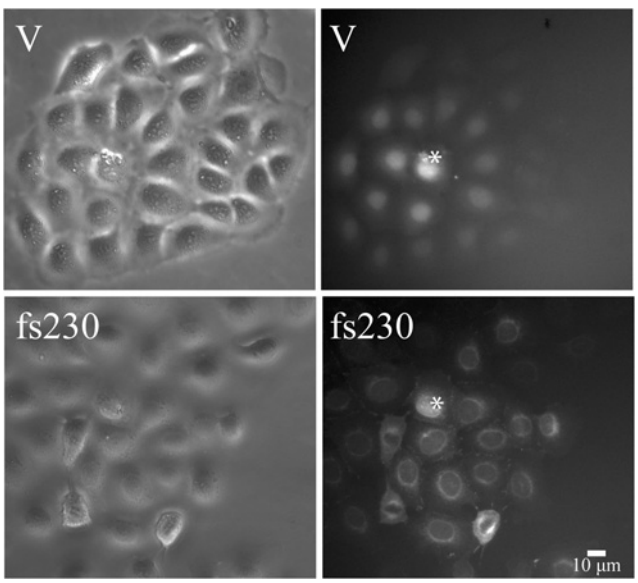

Figure S1 Microinjection of Lucifer Yellow into vector control and fs230-expressing REKs

A single cell was microinjected with Lucifer Yellow (asterisks) in either vector or fs230-mutant-expressing REKs. Lucifer Yellow was found to readily transfer to neighbouring cells in only the vector control cells. Phase-contrast (left panels) and fluorescent (right panels) images were acquired to visualize cell clusters and Lucifer Yellow dye transfer. Note that the GFP-tagged fs230 mutant was also detected in the fluorescent image.

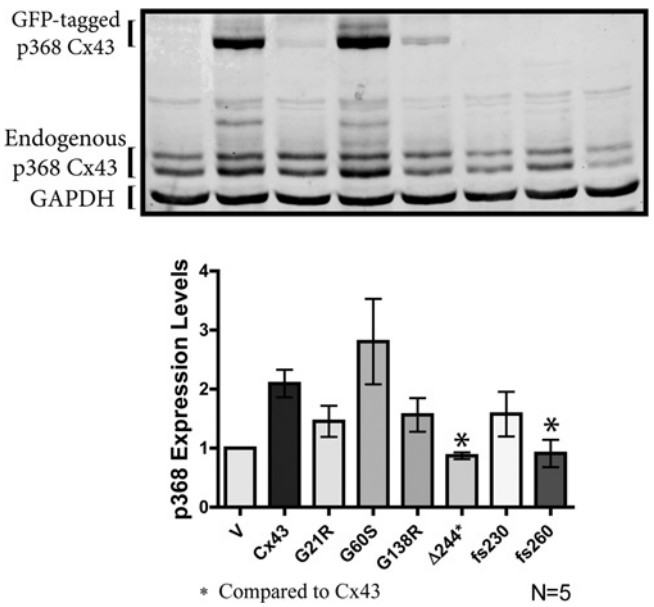

Figure S2 Western blot and quantification of the endogenous p368 phosphorylated species of Cx43

Western blots revealed a significant decrease in the p368 levels of Cx43 in both the fs260 and Δ244* cells when compared with full-length Cx43-expressing REKs. $*P<0.05$.

Received 27 January 2010/19 May 2010; accepted 1 June 2010
Published as BJ Immediate Publication 1 June 2010, doi:10.1042/BJ20100155

[1] To whom correspondence should be addressed (email dale.laird@schulich.uwo.ca).